Radiological and chemical risks by waste scales generated in the titanium dioxide industry

M.J. Gazquez[1)], J. Mantero [2)], F. Mosqueda [3)], I. Vioque[2)],

R. García-Tenorio[2)4)], J.P. Bolívar[3, *)]

[1)] *Department of Applied Physics, University of Cadiz, University Marine Research Institute (INMAR) Cadiz, 11510, Spain*

[2)] *Department of Applied Physics II, University of Seville, Spain*

[3)] *Department of Integrated Sciences, Center for Natural Resources, Health and Environment (RENSMA), University of Huelva, 21071, Huelva, Spain*

[4)]*Centro Nacional de Aceleradores, CNA, Universidad Sevilla- Junta Andalucía-CSIC, Sevilla, Spain*

* Corresponding author. Tel.: +34 959219793; fax: +34 959 21 9467. E-mail addresses: bolivar@uhu.es.

Abstract

Along the industrial process devoted to the production of titanium dioxide pigments by using ilmenite as main raw material, small residues amounts are generated, remaining clearly enriched in natural radionuclides and chemical pollutants. Between them, we can remark the scales enriched in both radium isotopes and lead, which are formed in the internal walls of pipes and some equipment. These scales are radiological anomalies that demand its mineralogical, elemental and radiometric characterization as a basis for a detailed radiological and toxicological assessment from the occupational and public point of view.

In this work, several scales collected in a TiO_2 pigment production plant in South of Spain have been mineralogically characterized by XRD, while information about their elemental composition and morphology have been obtained by applying the XRF and SEM techniques. In addition, radiometric determinations have been performed by gamma-ray and alpha-particle spectrometry.

The performed study indicates that the radiological doses received due to the scales by the workers performing its conventional activities are clearly lower than 1 mSv/y. Special dosimetric and chemical controls could be needed for the workers in charge of the maintenance labours (which include the removal of the scales) if these workers belong to an external company devoted to perform maintenance operations in several NORM industries.

Keywords: Major and Heavy Metals, Natural Radionuclides, External and internal doses, Radiological Risk, Chemical Risk.

1.Introduction

Is a well-known fact that any mining or minerals processing operation has the potential to increase the radiation dose received by individuals, due to the fact that all minerals and raw materials contain radionuclides of natural origin (García-Tenorio et al., 2015). The total radioactivity entering in the processes suffer its distribution among final products, by-products and residues, being the concentration and proportions found in each of these compounds very much dependent on the mineral/material treated and the process applied.

Some of these industrial processes, are characterized for generating small residues amounts along the production processes which present very high enrichment factors in some natural radionuclides and chemical elements.

Between these types of residues, we can remark the followings (García-Tenorio et al., 2015) (Godoy and Pettinati da Cruz, 2003):

(a) Scales: layers enriched in radium isotopes, and in some cases in ^{210}Pb, which are formed in the internal walls of pipes and equipment due to the precipitation of elements such as Ba and Pb in the form of sulphate compounds when a change in a physical variable affecting its solubility is produced along the process,

(b) Sludges: semi-solid material which is accumulated in deposits of several NORM industrial processes and that due to its very small grain size pass filtration steps accompanying the liquid fractions and experiment later on its decantation in the deposits where the liquids stay during long time intervals,

(c) Precipitator dust: very fine or volatilized material released in the processes of smelting and/or combustion of metals and minerals and that are trapped in cyclones and scrubbers before being released to the environment, and

(d) Filter-clothes: material used in filtration processes in several NORM industries that needs to be changed periodically due to their colmatation which reduce their filtration efficiency.

Due to their characteristics and their radionuclide content, these residues (scales, sludges, filter-clothes….) should be managed in most cases as low-level radioactive waste. Specialized waste management companies should take care of these residues, and equally important, only specialized maintenance workers should proceed to their removal from the production lines periodically due to its interference in the production process (IAEA, 2006). All the residues enriched in radium (^{226}Ra, ^{228}Ra) are, in addition, a source of gaseous radon (^{222}Rn, ^{220}Rn) fact that should be taken also in consideration especially during maintenance and management operations.

This type of residues can be found in a high number of different industrial processes. A very detailed list can be found in (IAEA, 2006). Only as examples, we can indicate that:

-Sludge samples can be found associated to the oil and gas production, the phosphoric acid production, the iron smelting and in water treatment plants

-Precipitator dust samples can be found associated to the thermal phosphorous production, to the fused zirconia production, to the niobium extraction and to all the metal smelting industry (Harvey et al., 1994; Penfold et al., 1999), and

-Filter clothes can be found associated to the phosphoric acid production and to the titanium dioxide production,

More in detail, due to its general higher radiological importance, we can indicate that scales heavily enriched in Ra and or Pb isotopes can be found also in a high variety of NORM industries. For example, in the petroleum extraction and production facilities, precipitation scales are generated in specific points of the production lines associated to abrupt changes in pressure and temperature and with typical concentrations for both ^{226}Ra and ^{228}Ra in the range 1 – 10^3 Bq/g, although concentrations up to 15.10^3 Bq/g can be reached (USEPA, 1993).

Another typical NORM industry where scales are generated is the phosphoric acid production where the raw material used (phosphate rock) contains high levels of natural radionuclides from the uranium series (1.0 – 1.5 Bq/g) (Bolivar et al. 2009) and where scales with an activity concentration of 4 – 12 Bq/g for ^{210}Pb and ^{226}Ra were reported (Beddow et al., 2006; Guerrero et al., 2020). Also, in the combustion of coal to produce heat and electricity some volatile radionuclides such as ^{210}Po can remain inside the burner kettles, being adhered to the walls and reaching concentrations over 100 Bq/g in the formed scales (Huijbregts and de Jong, 2000).

In this manuscript, the generated scales in a plant devoted to the production of titanium dioxide pigments located in Huelva (south west of Spain) were studied. In addition, also used filter-clothes along the same process have been analyzed. In this study, besides a radiometric/radiological evaluation a full mineralogical and elemental characterization were carried out in order to explain their formation process and obtain information about the potential presence of additional chemical contaminants to be taken in consideration during the industrial maintenance (removal) and management processes.

The TiO_2 production process presents a peculiarity. The raw material used for the pigment production contains enhanced amounts of radionuclides from both the uranium and thorium series. It can be expected to find radionuclides from both series simultaneously in the formed scales and in the used filters, being the total activity varying over time due to the breakage in these residues of the secular equilibrium in both series as will be discussed in the paper. Additionally, it is well known (IAEA, 2014) that the presence in the wastes from titanium dioxide industry of high concentrations of barium and lead is of concern. According to the World Health Organization (WHO, 2000) the primary routes of exposure to lead are ingestion of lead-contaminated substances and inhalation of lead particles that come from the maintenance operations inside the factory.

2. Description of the titanium dioxide pigment production process

A complete description of the titanium dioxide process applied in the Huelva plant can be found in a previous manuscript (Gazquez et al., 2009) and a general evaluation of the flow of radionuclides along the process can be found in (Mantero el et a., 2013). Here, only a summary will be included, in order to know in which steps of the process are used the filter-clothes and are formed the scales to be analysed. A complete study about Radiation Protection and NORM Residue Management in the Titanium Dioxide and Related Industries can be found in IAEA, 2012.

In short, the process, Figure 1, begins with the acid digestion of the raw material: until 2006 ilmenite (100%), a heavy mineral containing around 40-65% of titanium dioxide (Chernet, 1999), and since 2006 a mixture of ilmenite (80%), and titanium slag (20%) (a material generated in smelting ilmenite process (about 1700 ºC) with a low grade of titanium) (Pistorius and Coetzee, 2003). The digestion is carried out with concentrated sulphuric acid (around 95%), water (to activate the reaction) and recycled acid (around 65% concentration) (Gázquez et al., 2009).

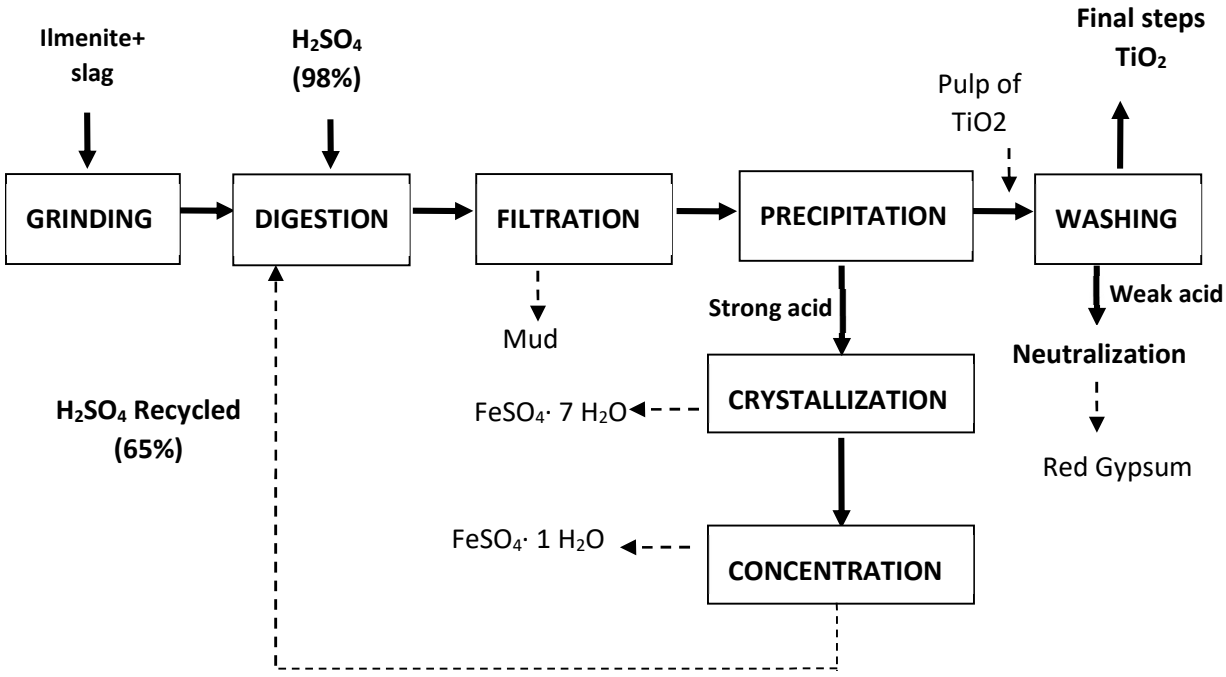

Figure 1 The manufacturing process of titanium dioxide pigment

The result of the digestion step is a liquid effluent enriched in titanil sulphate ($TiOSO_4$) and iron sulphate ($FeSO_4$), containing undissolved solids (mud). This mixture is then sent to a clarification tank in order to separate both fractions, being afterwards treated the separated mud as residue.

Associated to this digestion process it has been demonstrated that a big proportion of the U and Th originally present in the raw material pass to the liquor, while the majority of the Ra-isotopes in the form of insoluble sulphates are associated to the mud (Gazquez et al., 2011; Mantero et al., 2013, Contreras et al., 2014).

The titanium liquor is then concentrated and hydrolysed in order to produce a hydrated titanium dioxide precipitate. This titanium dioxide hydrate in solid form (TiO_2 cake) is separated from the remaining liquor through filtration using vacuum filters (known as Moore filters). The remaining liquor is commonly known as “strong acid", contains around 20–25% H_2SO_4, and it is treated independently in a parallel process as it will be detailed later on.

In this step of titanium dioxide hydrate generation by concentration and hydrolysis, it has been demonstrated that the majority of the U and Th present in the original liquor in dissolved form remains in the strong acid, being transferred to the titanium dioxide cake only minimum amounts of these radionuclides (Mantero et al., 2013).

After filtration, the resulting TiO_2 cake is washed with water to remove the remaining impurities, being obtained a solid phase containing TiO_2 and a liquid phase usually called “weak acid solution” (1 – 1.5% H_2SO_4), see Figure 1. Then, the washed hydrated titanium dioxide is sent to the final steps for conditioning the commercial TiO_2 pigment, after the removal of the residual water and H_2SO_4 remnant.

The hydrated titanium dioxide after washing is free of radionuclide impurities, which stays in the weak acid solution (Mantero et al., 2013). This generated weak acid solution is treated independently in another parallel process that also will be detailed in a coming paragraph.

The so-called “strong acid” (20%-25% H_2SO_4), separated after the initial TiO_2 cake precipitation and containing dissolved iron, is submitted to a process where two co-products are generated: first the strong acid is pumped into batch cooling crystallizers, being formed iron sulphate heptahydrate ($FeSO_4 \cdot 7H_2O$), usually known as copperas, and afterwards, once the copperas is separated, the resulting liquor is concentrated in different evaporative steps, generating ferrous sulphate monohydrate ($FeSO_4 \cdot H_2O$) and a recycled weak acid (liquid phase), which will be used in the digestion step.

The radioactive content of copperas is less than unperturbed soil (around 40 Bq/kg) from the uranium and thorium series, (UNSCEAR 2008) while in the monohydrate precipitate, the radioactive content is around 500 Bq/kg for ^{228}Th and ^{228}Ra (Mantero et al., 2013). The great majority of U and Th originally present in the strong acid is accumulated in the monohydrate.

The generation of the copperas by crystallization is caused by vacuum when the boiling temperature is 20°C, causing saturation of the solution and precipitation of the ferrous sulphate heptahydrate, separated by centrifugation. In this step, and due to sharp changes in pressure, scales are formed and accumulated in the walls of the so-called “crystallizers”, which are analysed in this work.

Concerning the weak acid generated in the washing of the titanium dioxide cake, simply indicate that is submitted to a neutralization process where a residue called red-gypsum is generated. The main mineralogical composition of this residue is gypsum (Gazquez et al., 2013) with activity concentration of ^{226}Ra and ^{228}Ra is around 20 and 70 Bq/kg (Mantero et al., 2013).

In summary, two types of by-products are generated in the titanium dioxide industry (copperas and monohydrate) (Gazquez et al.,2009), and two types of waste (undissolved mud and red-gypsum) are generated. In addition, this article will demonstrate that in two

stages of this industrial process (Moore filters zone and scales from treatment of strong acid) natural radioactivity is concentrated and they constitute hot spots for external exposure and inhalation.

3. Materials and methods

3.1 Materials and sampling

Highly radioactive scales in the crystallization step were identified and collected during maintenance works. Scales collected in the crystallizers of the Huelva plant in two different collection dates separated between then more than 10 years were analysed for evaluating how the use of titanium slag in addition to the ilmenite as raw material is reflected in changes in mineralogy, elemental and radioactive composition of the scales. Scales collected in 2006 when the raw material processed was exclusively formed by ilmenite, and collected in 2016 when the raw material was a mixture of ilmenite and titanium slag were analysed.

A representative sample of a Moore filter, and a scale formed in a pipe of the production process has been also characterized.

The complete set of samples analysed in this work are compiled in Table 1.

Table 1. Descriptive summary of the collected samples.

CODE	SAMPLE	DESCRIPTION
CS1	Crystallizer Scale	Sampled collected from the crystallizer in 2006.
CS2	Crystallizer Scale	Sampled collected from the horizontal crystallizer in 2016.
CS3	Crystallizer Scale	Sampled collected from the vertical crystallizer in 2016.
MF	Moore Filter	Vacuum filters used by separation of precipitated hydrated TiO_2 from the mother liquor.
IS	Internal Scale	Scale taken from inside a titanium dioxide production pipe.

3.2 Methods for physical and chemical characterization

3.2.1 Techniques based on X-rays

3.2.1.1 X-Ray Diffraction (XRD)

The mineralogical analyses were carried out using the X-ray diffraction (XRD) technique. Measurements were performed, using a Bruker D8 Advance A25(D8I-90) instrument. Cu Kα radiation filtered by a Ni film and excited with a 30 mA intensity and 40 kV tension was used. The exposure time at each point was 0.1 s. The lineal detector was Lynxeye by Bruker. A semi-quantitative method, Reference Intensity Ratio (RIR), was used for the mineralogical quantification. This measurement system has a detection limit of around 1%.

3.2.1.2 X-ray Fluorescence (XRF)

The elemental compositions of the scales were determined via wavelength dispersive X-Ray fluorescence (WDXRF) by using an AXIOS system from Panalytical Company. This device has a Rh tube and is equipped with two detectors, a flow counter and a scintillation counter. This equipment allows qualitative and quantitative chemical analysis from O to U in a wide range of concentrations from major components to traces, reaching typical detection limits of 0.1 ppm.

3.2.1.3 SEM-EDX

Information about the morphological and elemental compositions of the samples were also performed by using a JEOL 6460LV scanning electron microscope (SEM) with acquisition of digital images in both secondary (SEI) and backscattered (BEI) modes (maximum resolution 3.5 nm). This device was coupled to an EDX microprobe. It has three types of detectors for receiving the different signals from the sample. The one used to detect secondary electrons is a scintillator with the Everhart-Thornley configuration;

for backscattered electrons a semiconductor detector with the same configuration, Everhart-Thornley, is used; and the energy dispersion X-ray detector is a lithium-doped silicon semiconductor detector, fitted with an ATW2 beryllium window (resolution 137 eV at 5.9 keV). The semi-quantitative elemental analysis was performed using Oxford INCA software.

3.2.2 Alpha-particle spectrometry.

U-isotopes (^{238}U, ^{235}U, ^{234}U) and Th-isotopes (^{232}Th, ^{230}Th and ^{228}Th) alpha-emitters were determined by applying this technique in independent samples in order to gain as much information as possible. For U/Th isotopes determination, small amounts of scales (~ 0.20 g) were used and three replicates were measured for each sample in order to evaluate if there are inhomogeneities. The reported results with this technique is the mean and its associated uncertainty evaluated as the standard deviation of the three measurements. A total of 15 aliquots (5 samples x 3 replicates) were treated.

Initially, a total digestion with HF and a solution of (HNO_3: HCl ratio 1:3) or "aqua regia" (followed by a complexation process with boric acid) was applied in a commercial microwave, model Multiwave 3000 from Anton Paars equipped with 8 vessels.

These scale samples, are far from being considered as "typical" in a laboratory mainly devoted to radiochemistry of environmental samples analysis. In fact, the initial U/Th procedure applied in some of these scales started with the digestion of 1g of sample and spiking with 1 g approximately of U (^{232}U of 116 mBq/g) and Th (^{229}Th of 75 mBq/g) of tracers to the digested sample. This solution followed a sequential extraction of Th first and U later according to Lehritani (Lehritani et al., 2012) what produced useless alpha sources (huge alpha peaks with negligible amount of isotopic tracers were found in few

minutes of counting time, complex determination of ^{228}Th due to additional contribution of tracer ^{232}U, etc). As a consequence, it was decided to decrease the amount of scale treated and apply a dilution process to avoid problems in the way it is described just below.

In the revised and final method, each aliquot of 0.2 g each was digested using the mentioned microwave system. After the digestion, 20 g/sample of solution was generated and distilled water was added until c.a. 100 g. This solution was split in several fractions: For proper U-isotopes determination, half of the diluted solution (~ 50 g/sample) was spiked with 1g of ^{232}U tracer and then distilled water was added again up to 200 g. In case of Th-isotopes, only ~1 g out of the 100 g solution was spiked with 1g of ^{229}Th tracer and then distilled water was added up to 200 g in the same way than the U-isotopes fraction.

So far, two independent solutions of 200 g (one for U-isotopes containing 0.1g of scale sample and a second one for Th-isotopes containing 0.002 g of sample) were generated from each 0.20 g of scale aliquot. This high dilution, in the case of Th, was forced due to the very high activity concentrations of ^{228}Th (daughter of ^{228}Ra), in order to work with proper ^{228}Th/^{229}Th activity ratios. The U and Th solutions were then submitted to an iron hydroxide precipitation process followed by a liquid-liquid solvent sequential extraction (based in the use of Tributyl Phosphate, TBP) to isolate Th and U isotopes and to separate them from other alpha interferences (Lehritani et al., 2012). Th fraction still need and additional purification procedure where chromatographic resins (UTEVA resins from Triskem) were used (Mantero et al, 2019).

Finally, U and Th alpha sources were generated by electroplating each fraction onto steel disks using a solution of $(NH_4)_2SO_4$ (Hallstadius, 1984).

U and Th alpha sources were measured in a Canberra Alpha-Analyst system using passivated implanted planar silicon (PIPS) detectors with independent counting chambers

for U and for Th isotopes. Typical measurement conditions with this system: 1 g of sample, 170000 s of measured time and assuming an average 50% chemical recovery (Y) provide a minimum detectable activity (MDA) around 2–3 mBq/kg. Usually measurement times for background (t_B) and sample (t_S) are not the same. The MDA value is assessed according to Eq [1] with 95% confidence level [Hartwell 1975, Genie 2000, 2004].

$$MDA\left(\frac{Bq}{g}\right) = \frac{2.71+3.29\sqrt{N_B+\frac{N_B t_B}{t_S}}}{t_S \cdot \varepsilon \cdot P \cdot Y \cdot M} \qquad \text{Eq 1}$$

Where N_B are the net counts in the Region of Interest (ROI) of the background spectrum, ε the efficiency detection (around 25% with 5 mm source-to-detector distance) for the alpha source, P the probability emission (around 100 %) in case of alpha emitters and M the mass (in g) of the sample.

Despite the high activity concentration of some radionuclides in these samples, due to the applied dilution process, measuring times of c.a. 100000 s were applied to these diluted aliquots.

3.2.3 Gamma spectrometry

Gamma measurements were carried out using an XtRa coaxial germanium detector (Canberra) with 42.1% relative efficiency and 1.95 keV resolution (for the ^{60}Co gamma emission at 1332 keV). Due to the small available sample amount, scales samples were packaged in two different Petri disks—P33, a container with 33 mm diameter and 10 mm high, and a P5 container, 20 mm diameter and 15 mm high. For efficiency calibration, U-ore and Th-ore reference materials from IAEA were used, avoiding in this way the need to apply true coincidence-summing corrections. In addition, low energy gamma emitters

(mainly ^{210}Pb and ^{234}Th) were corrected for self-absorption effect. The procedure of the gamma spectrometry is previously described by Mantero (Mantero et al., 2015).

Radioisotopes, such as ^{226}Ra or ^{228}Th, are reported assuming secular equilibrium with their daughters after 3 weeks of storage before being measured. Some isotopes, such as ^{214}Bi, ^{228}Ac or ^{208}Tl, will have several lines evaluated; in these cases, the activity concentration reported will be the average of all their measured γ-lines followed by the standard deviation with 1-sigma criteria (k=1). These samples were measured far away from the detector (c.a. 20 cm source-to-detector distance) due to the high gamma activity concentration of several radionuclides, decreasing the detector dead time from 10-20% in the closer geometry (usually 1 cm from the window) to dead time below 0.5% in all cases. With this geometrical configuration, measurement times of these samples ranged from 50 to 150 ks Typical MDA for this system ranges from 0.2 to 12 Bq/kg. Used gamma lines and MDA for the different radionuclides are shown in Table S1 of supplementary material, (Mantero et al 2019).

3.2.4 External Dosimetric analysis

An extensive and detailed external dosimetric survey was carried out in the Huelva plant throughout the titanium dioxide manufacture process, in order to identify the points or areas of radiological concern. A universal monitor (model UMo LB 123 from Bertold) designed specifically for the measurements of low dose rates was used. It is equipped with a probe certified by the Deutsches Institutfür Normunge.V. (the German Institute for Standardization), working in proportional mode. The system allows the measurement of both dose rate and integrated dose.

3.2.5 Internal doses by aerosol inhalation

The estimation of internal doses by aerosol inhalation, based on the International Atomic Energy Agency (IAEA) criteria and values (IAEA, 1999, 2004 and 2014) could be done through the formula

$$\mathbf{E}\ (\mathrm{Sv}) = \mathbf{P}\ (\mathrm{g})\ \sum_j \mathbf{Cj}\ (\mathrm{Bq/g})\ \mathbf{hj}\ (\mathrm{Sv/Bq}) \qquad \text{Eq 2}$$

where E is the dose (Sv) due to inhalation of P(grams) of aerosols containing different natural radionuclides with activity concentrations Cj and dose coefficients for inhalation of radionuclides hj (Sv/Bq) taken from the Directive 2003/88/EC.

Equation 1, has been mainly used in this work associated to the possibility of aerosol inhalation in the maintenance works performed for the collection of the three scales collected in the crystallization area of the factory (samples CS1, CS2, and CS3).

4 Results and discussion

4.1. Mineralogical composition

The XRD diagram corresponding to some of the scales analysed are shown in Figure S1 of supplementary material. In all the samples analysed it was observed that the crystalline fraction content is dominant, higher than 75%, in agreement with its origin and its formation process. This special characteristic was particularly important in the scales formed in the crystallizers as expected.

The scales collected in the crystallizers (codes CS1, CS2 and CS3, Table 1) were composed exclusively of anglesite (lead sulphate), Figure S1 A) of supplementary material. Lead sulphate is highly insoluble, being particularly enhanced its co-precipitation with other group II elements (for example, barium and radium sulphates), in the process of pressure and temperature changes as occurs in the crystallizers.

It is necessary to remark that most of the lead initially contained in the raw material it is not solubilized in the initial digestion step remaining in the first residue generated in the process (undissolved mud), see Figure 1. Only a quite low proportion of lead and group II elements are present in dissolution in the strong acid solution submitted to the crystallization process. However, it is important to take into account that the scales precipitation in any industrial process occurs continuously over time and, therefore, the low concentration of lead sulphate remnant through the process precipitates and accumulates in the crystallizers, where the high vacuum promotes its precipitation.

A similar trend occurs for the internal scales (code IS, Figure S1 B of supplementary material), with barium lead sulphate as the main crystalline phase at 81% and around 20% aluminium iron titanium oxide.

4.2. X-ray fluorescence

The percentages of major chemical elements (%) in the collected samples are shown in Table 2.

The samples collected in the crystallizers (CS1, CS2 and CS3) are mainly composed by Pb (46, 35 and 32%, respectively), as expected from their previously determined mineralogical composition (anglesite or lead sulphate). In fact, the Pb/S ratio in the three crystallizer scales, 6.66, 5.62 and 6.32, respectively, are in good agreement with the theoretic mass ratio in the lead sulphate, which is 6.46

In the Table 2 is also clearly reflected that elements such as Pb, Ba, Ca, Ce, Fe, La, Si and Sr have higher concentrations in the sample CS1, collected when the raw material used in the industrial process was only ilmenite, than in the samples CS2 and CS3, collected when the raw material used was a mixture between ilmenite and titanium slag (Gázquez et al., 2009; Mantero et al., 2013).

In general, the mentioned elements have higher concentrations in ilmenite than slag. For example, the mean concentration of Fe in ilmenite is 44%, while in slag samples it is clearly lower, around 10% (Gázquez et al., 2009), while rare earth elements, such as La and Ce, are mainly contained in the pseudorutile mineral phases that are directly associated with the ilmenite ore (Pownceby et al., 2008). Also the scale CS1 has higher lead concentration (24 and 30% respectively) than scales CS2 and CS3, a fact that as was indicated previously is compatible with the change of raw material in the industrial process. Previous studies in the industry showed that the concentrations of Pb were 135 and 36 mg/kg in ilmenite and slag samples, respectively (Gázquez et al., 2009). The different proportions in the elemental composition of the crystallizer scales is totally compatible with the modification of the feed raw material carried out in 2006.

Table 2. Concentrations (%) of major elements by XRF in the collected samples.

	CS1	CS2	CS3	MF	IS
Al	0.07	0.04	0.01	0.06	2.25
Ba	4.60	3.60	3.91	0.38	13.1
Ca	0.74	0.07	0.08	0.06	1.64
Ce	0.60	0.28	0.24	<0.01	<0.01
Cl	0.10	0.10	0.16	0.12	0.71
F	<0.01	<0.01	<0.01	<0.01	0.43
Fe	2.84	1.00	0.49	0.19	18.1
K	0.24	0.20	0.25	0.01	1.41
La	0.81	0.41	0.46	<0.01	<0.01
Na	0.09	<0.01	0.06	0.06	0.51
O	27.9	18.4	17.6	64.1	20.4
Pb	46.1	35.4	38.2	1.26	18.1
S	6.92	6.30	6.04	1.34	5.02
Si	3.19	1.13	1.27	0.18	2.42
Sn	0.15	0.05	0.13	0.44	0.16
Sr	1.35	0.71	0.77	0.04	0.60
Ti	4.24	5.44	4.42	32.2	4.47
Zn	<0.01	0.02	0.03	0.10	9.85

It should be noted that he concentrations of barium obtained in the same scales were high, with 4.6, 3.6 and 3.9% for CS1, CS2 and CS3, respectively. Taking into account the insolubility of both barium and lead sulphate, this result is not surprising. The higher Z elements in group II follow the lead in the precipitation/formation of the crystallizer scales. The concentrations of other elements, such as Al, Cl, Ti, K, Sn, Ti, and Zn, did not present significant differences between samples collected in different years.

The pipe scale analysed shows high concentrations of Ba, Pb and S, with 13, 18 and 5%, respectively. These results agree with the results obtained by XRD indicating the presence of barium lead sulphate. And, additionally, a considerable percentage of Al, Fe and Ti was present in this sample, with 2.25, 18.1 and 4.47%, respectively, in good correspondence with the aluminium iron titanium oxide crystalline phase observed in the XRD measurement, see Figure S1 B) of supplementary material.

In the pipe scale, it is also important to note the high concentration found for Zn (9.85%); although this element does not have an important concentration in the raw material (Klepka et al., 2005; Gázquez et al., 2009), the continuous precipitation of metals in the internal walls of pipes causes the concentration of this metal that reach values even higher than titanium. Zn compounds remains in an amorphous state because its presence was not detected by XRD.

Finally, attending to the results show in Table 2, we can indicate that the main element found in the material adhered to the collmated Moore Filter is titanium (32.2%), because TiO_2 particles become trapped in the filter during the filtration process of the titanium dioxide hydrate, where it is separated from the strong acid. In addition, concentrations of 0.38, 1.26 and 1.34 % for Ba, Pb and S, respectively, suggest that also that some lead and barium sulphate compounds could remain in the filter.

4.3. Scanning electron microscopy (SEM)

The analysis of the samples included in this study was complemented though the application of the SEM-EDX technique to the crystallizer and internal scale samples and also to the particles obtained by scraping gently the surface of the Moore filter.

A representative SEM image of the crystallizer scales is shown in Figure S2 of supplementary material. From this figure, and taking into account the EDX analysis, it was possible to confirm that these crystallizer scales are mainly composed of Pb, S, Ba and Ti, with other elements, such as K, Fe, Si and Sr, present in lower concentrations. This information agrees with the data shown in Table 2, obtained by XRF and with the information gained by XRD, where it was concluded that the only crystalline phase in these samples was anglesite.

In relation to the pipe scale, Figure S3 of supplementary material, the general composition agrees with the obtained by XRF, Table 2. The EDX analysis indicates that the main constituents are Pb, Ba, S, Ti, Fe and Zn, with other elements, such as Al, Sr, Sn and Si, in trace concentrations. This result is also compatible with the results obtained by XRD, with the presence, in the crystalline phase, of barium lead sulphate and aluminium iron titanium oxide. The presence of high concentrations of Zn, previously commented in the evaluation of the XRF results, is confirmed.

The high concentration of Pb, particularly for CS samples could be of concern, remembering that WHO point out that the primary routes of exposure to lead are ingestion and inhalation of lead particles. It should be taken into account that the annual average lead level in air should not exceed 0.5 $\mu g/m^3$. On the other hand, the concentration of Ba in the IS sample should be taken also with precaution because the level in air should not exceed 0.5 mg/m^3 (ATSDR, 2007). This aspect will be deeply analysed in the section 4.5, where the radionuclide inhalation doses are discussed because the inhalation rates and

occupancy factors are the same that the used for radionuclides. The chemical determinations will allow to perform a complete inhalation risk assessment.

Finally, the surface of the Moore filter (MF) was gently scraped, obtaining a few grams of sample, which were analysed by SEM-EDX. The obtained results, see Figure 2, indicates first that the particle size is highly homogeneous (between 20–40 microns) which can be related to the characteristics of the filter and the fact that the analysed particles were trapped on it.

The particles shown in Figure 2 present a non-uniform composition. The EDX analyses indicate that the particles marked with numbers 1 and 2 are quartz crystals with impurities of Ti, Fe and Al, while particle 3 is rutile (TiO_2), mainly composed of Ti and O, and Particle 4 is mostly composed by Cu and S, with traces of Ti, Si and Fe. Particles, 5, 6 and 7 show a uniform composition and similar morphology, where the Zn and O appears as main elements. Finally, Particle 8 contains significant percentages of Pb, Ba, Ti and S, and traces of Zn, Fe and Si. The high heterogeneity of the samples was expected, considering its origin in a filtration process.

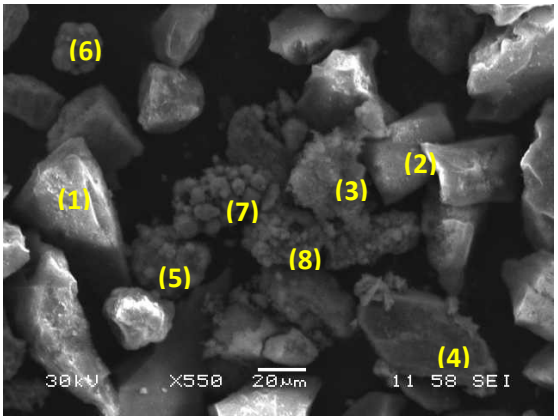

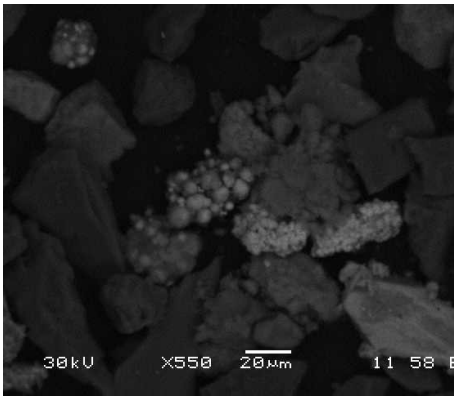

Points	C	O	Al	Si	S	Cl	Ti	Fe	Cu	Zn	Ba	Pb
1	5.3	57.5	0.18	36.0	-	-	0.51	0.54	-	-	-	-
2	-	52.2	-	47.8	-	-	-	-	-	-	-	-
3	-	46.9	-	1.14	-	-	51.2	0.71	-	-	-	-
4	7.8	9.0	-	0.56	20.1	-	0.9	1.29	59.7	-	-	-
5	6.3	37.5	3.5	9.6	2.7	2.97	0.97	1.05	-	34.3	-	-
6	6.3	34.4	5.8	11.3	-	0.73	0.3	1.34	-	39.8	-	-

7	-	7.3	-	1.01	-	0.65	0.69	1.85	-	88.0	-	-
8	5.2	37.0	-	0.94	5.6	-	18.3	1.78	-	0.51	22.7	8.0

Figure 2. SEM specific analysis of several particles from the Moore filter sample, obtained in both secondary (SEI) and backscattered (BEI) electron imaging modes and elementary composition of the particles (%), evaluated by EDX.

4.4 Radiometric determinations

In Tables S2 and S3 of supplementary material are compiled the radiometric data obtained for each sample at the time of the application of the different measuring techniques, while Table 3 compile the results for the key radionuclides after correction at the time of sample collection, because there are the essential ones in order to evaluate the potential doses by inhalation received by the maintenance workers during the scales removal. These corrections in some samples and for some radionuclides are significant since, as was commented previously, the time elapsed between the sample collection and measurements was more than one half-life of the involved radionuclides, specially ^{228}Ra, ^{228}Th, and ^{210}Pb.

Table 3.- Activity concentrations (Bq/g) of the key radionuclides determined in all the samples, corrected at the time of collection (t_0).

Sample	^{226}Ra	^{210}Pb	^{228}Ra
CS1	121 ± 6	102 ± 13	185 ± 8
CS2	448 ± 24	317 ± 23	2192 ± 284
CS3	190 ± 8	256 ± 25	966 ± 134
MF	14.4 ± 0.6	3.5 ± 1.1	64 ± 6
IS	1281 ± 40	1531± 82	169 ±7

In all the analysed samples a clear distinction in the activity concentrations can be observed between nuclides such as ^{238}U, ^{234}U and nuclides such as ^{226}Ra, ^{228}Ra, and ^{210}Pb

with activity concentrations of these last ones in factors 10^2-10^5, specially the IS sample, as can be seen in Tables S2 and S3 of supplementary material.

A special case is the case of ^{228}Th, observed in concentrations comparable to its parent ^{228}Ra due to the time elapsed between the measurement and the collection of the sample. The previously commented tendency to accumulate Ra and Pb isotopes in these deposits is evidenced (Landa, 2007).

At this stage it is worth to mention that the determinations performed in all the samples of Th-isotopes alpha emitters (^{230}Th, ^{232}Th and ^{228}Th) does not allow the precise determinations of the ^{232}Th and ^{230}Th activity concentrations, because the levels of ^{228}Th (and of the tracer ^{229}Th) were several orders of magnitude higher, as evidenced in Figure S4 of the supplementary material. In the spectrum of this Figure, is observed that the peak of ^{228} Th is much more relevant that ^{232}Th peak and ^{230}Th. The ^{228}Th/^{232}Th counts ratio is around 550 while ratio ^{228}Th/^{230}Th is 100. This fact makes not possible the determination of ^{232}Th and ^{230}Th with enough precision to be reported, although it is evident that the activity concentrations of ^{232}Th and ^{230}Th can be considered negligible in comparison with the activity concentrations of ^{228}Th (more than 2 orders of magnitude).

For a proper evaluation of the results obtained at the time of measurement for the radionuclides of the Th-series, we can then estimate in a first approximation that at the time of sampling collection the activity concentrations of ^{232}Th and ^{230}Th are negligible, being present at initial time (t_o) only ^{228}Ra. From the time of collection, the ^{228}Ra will be decaying with its own half-life, while the activity of its daughter ^{228}Th follows a well-defined evolution over time deduced from the resolution of the Bateman's equations in the sub-series ^{228}Ra-^{228}Th, see Figure 3.

Under the mentioned assumption reflecting the only initial presence of ^{228}Ra, it is straightforward to calculate the initial activity of this nuclide in all the samples only,

taking into account the time elapsed between the sample collection (initial time) and the time of the measurement. In addition, once the initial activity of ^{228}Ra in each sample is known, to stablish for each individual sample the temporal evolution of the sub-series ^{228}Ra-^{228}Ac-^{228}Th is immediate, allowing to check if the assumptions taken could be considered valid, looking how coherent are the experimented ^{228}Th determinations performed, by gamma and alpha spectrometry with the estimated values from the calculated curves. In Figure 3, we show the estimated temporal evolution of the activity concentrations of ^{228}Ra and ^{228}Th for two of the samples analyzed in this work, and how the ^{228}Th experimental values reasonably fits with the estimated ones, supporting the hypothesis taken. In figure S5 of supplementary material are shown the temporal evolution of the activity concentrations of ^{228}Ra and ^{228}Th for the rest of the samples.

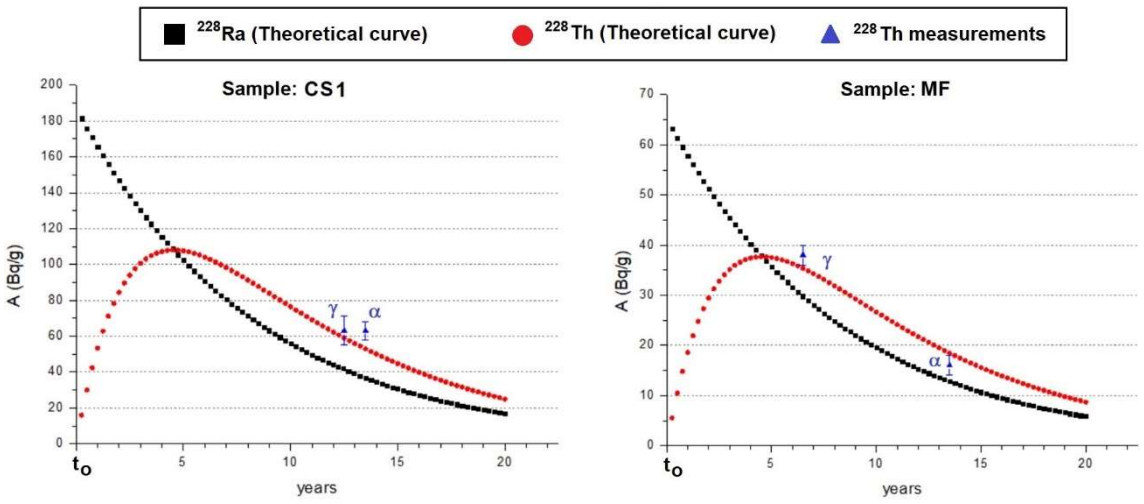

Figure 3. Estimated temporal evolution of the activity concentrations of ^{228}Ra and ^{228}Th of two of the samples analyzed, together with the values obtained for ^{228}Th in the experimental measurements by gamma-ray and by alpha-particle spectrometry.

In relation to the U-series radionuclides the two key radioisotopes to have in consideration are ^{226}Ra and ^{210}Pb. Their activity concentrations are several orders of magnitude higher

than the observed ones for the other long-live radionuclides as ^{238}U, ^{234}U and ^{230}Th. Due to the very long half-life of ^{226}Ra (half-life = 1602 y), for this radionuclide no correction time is needed. On the contrary, for ^{210}Pb (half-life = 22.3 y), daughter of ^{226}Ra, it is needed to apply the Bateman's equation for calculating its activity concentration in the sampling time (t = 0), $A_d(0)$, according to the equations:

$A_P = \lambda_p N_p$ Eq 3

$A_d = \lambda_d N_d$ Eq 4

$$A_d(t) = A_p(0)\frac{\lambda_d}{\lambda_d - \lambda_p}\left(e^{-\lambda_p t} - e^{-\lambda_d t}\right) + A_d(0)e^{-\lambda_d t} \qquad \text{Eq 5}$$

, where "p" is the ^{226}Ra and "d" the ^{210}Pb, t is the elapsed time from sampling to the counting, $A_d(t)$ the ^{210}Pb activity in the counting time, which is known, and lambda the corresponding decay constants.

Taking into account the high activity concentration of ^{226}Ra (upper than 400 Bq/g for CS2), the concentration of ^{222}Rn (daughter of ^{226}Ra) should be analyzed. This measurement was carried out in the crystallizer where the CS2 was taken, by using a Radon Scout professional equipment (at 100 Bq/m³ gives a 17% statistical error (1σ) for 3 h of counting). The first measurement was performed with closed doors of the crystallizer (CS2), reporting values near to 10000 Bq/m^3, one order of magnitude upper than the limit (1000 Bq/m^3) given by National legislation for exposed workers (Technical Instruction of Nuclear Safety Council, 2011). This Instruction point out that levels of radon lower than 600 Bq/m^3 in working places it is no necessary a radiological control. The second experience was carried out with the open doors, reporting at the steady state concentrations around 1000 Bq/m^3, which need radiological control since they are higher than the reference threshold (600 Bq/m^3). Therefore, finally was developed an experience by using forced ventilation with a standard fan with the open doors of the crystalliser, and

a radon stationary radon concentration of 200 Bq/m^3 was measured, which is below of the previous cited threshold (600 Bq/m^3). For that reason, a forced ventilation will be necessary during the maintenance operations.

4.5 Risks assessments

Table 4 compiles the external gamma dose rates (over background) along the TiO_2 industrial process.

Table 4. External gamma dose rate above background along the whole Titanium dioxide production process. Background of the area: 0.09 µSv/h.

Site	µSv/h
Open area for storage of raw material (ilmenite)	0.22 - 0.39
Digestion area	0.11 - 0.22
Un-attacked separation area	0.10 - 0.22
Storage of Moore filters	2.00 - 2.50
Tank of leaching pulp	0.11
Storage tank of strong acid	0.45
Copperas formation. Horizontal crystallizer A	0.25 - 3.50
Copperas formation. Horizontal crystallizer B	0.30 - 12.60
Pipe between crystallizers	2.60 - 5.10
Copperas formation. Vertical crystallizer A	0.18 - 0.54
Copperas formation. Vertical crystallizer B	0.16 - 0.62
Thickener tank for copperas	0.22 - 0.26
Copperas storage	0.08

The survey carried out evidenced that the industry devoted to the production of titanium dioxide pigments is a NORM industry, with values of the external gamma doe rates above

the background along the whole process and with clearly higher values in the two following specific zones:

a) The crystallization area where the scales studied in this work are formed over time accumulating Ra and Pb isotopes at this stage of the process (most of the Ra and Pb entering in the process, leave it in the initial digestion step associated to the undissolved mud treated as residue). These scales are collected from the crystallizers with a time separation of several months and contain all the Ra and Pb precipitated during this time interval.

b) The storage area where the Moore filters, after colmatation, are stored. In an accumulation process, these filters retain in their pores fine particles enriched in Ra and Pb in the process of separation after the digestion step. Insoluble Ra-Pb sulphates, as deduced from the XRF analyses, are trapped in the filter pores.

In the crystallizers, external gamma dose rate up to 12.6 μSv/h were found, while in the area devoted to the storage of Moore filters the higher values found reach 2.50 μSv/h, being important to remark in order to find some correlation between these values and the radiometric data that in the case of the scales collected in the crystallizers and in the connexion pipe, the radiation is attenuated because are inside these devices/components, while in the case of the Moore filters the external radiation measurements correspond to the generated by a group of several filters stored in the measured area.

In most of the areas of the factory the external gamma dose rates are clearly lower than 0.5 μSv/h, fact that assuming an occupational factor of 2000 hours per year implies that the dose rate received by the workers are moderate, remaining well below the reference value of 1 mSv/y. The clearly higher values observed in the crystallization and filter storage areas have a minimum influence in the annual external doses received by the

workers because correspond to limited zones characterized by a very low occupancy factor. Only the maintenance workers removing the scales from the crystallizers could receive higher external doses, but not reaching 1 mSv/y due to the limited short time needed to perform this task (around 80 hours) and to the very low frequency and time maintenance required (once per year, maximum).

Some concern could exist about the doses by inhalation received by the maintenance people during the removal of the scales from the crystallizers. Taking into account the key radionuclides (radionuclides with clearly higher activity concentrations) ^{226}Ra, ^{210}Pb, ^{228}Th and ^{228}Ra at the moment of removal and assuming, in a conservative way, secular equilibrium between ^{210}Pb and ^{210}Po at the moment of sample collection, Equation 2 (section 3.2.5) was applied to the scales samples, see Table S4 of the supplementary material.

We can see that the during the maintenance labour could be inhaled, as maximum, 317, 19, 34, 72, and 714 mg for CS1, CS2, CS3, IS and MF samples, to ensure that the annual committed dose for workers due to the inhalation of particular matter is lower than 1 mSv/y.

An in relation to the chemical risks, to comment that stable lead has a recommended limit recommended by WHO of 0.5 μg/m^3 as annual average, and assuming an occupational factor of 2000 hours per year plus an inhalation rate of 1.5 m^3/h, (ICRP 66, 1994) it is deduced that the maximum quantity of Pb to be inhaled to not overpass the WHO limit is 1.5 mg per year. Taking into account the concentration of lead 46, 35.4, 38.2, 18.1 and 1.26% for CS1, CS2, CS3, IS and MF samples, see Table 2, it is immediate to deduce that maximum values of 3.3, 4.3, 3.9, 8.3 and 125 mg of scales could be inhaled within the limit of 1.5 mg/year, previously calculated. In the case of Ba, the concentration of this element in the IS sample is 13%, but because the maximum allowed level in air is 0.5

mg/m^3 annually (ATSDR, 2007) a equivalent value of 1.5 g of Ba/year can be inhaled, a value 10^3 higher than for Pb, indicating that from chemical point of view, the most important toxic element to take into account will be Pb.

The comparison of the radiometric with the chemical risks conduit to a clear conclusion: in the case of the scales the chemical/toxicological risk due to inhalation of stable Pb is higher than the radiological one.

This conclusion is reflected in the radiological (Cr) and chemical (Cc) maximum particulate matter concentration allowed to be inhaled in the maintenance works which has been calculated assuming 80 hours per year of work in the maintenance operation and inhalation rate of 1.5 m^3/h, see Table S4. In all the samples the maximum allowed particulate matter concentration values are 3 to 10 times lower attending to toxicological/chemical considerations in comparison with the radiological ones.

For that reason, the use of protective masks and to work with wet scales is imperative because it would significantly reduce the impact of the inhalation route as a way of potential risk for the maintenance workers.

The management of these scales after removal from the process, and the associated radiological implications are out of the scope of this work.

5. Conclusions

The scales collected along the TiO_2 industrial process are found mostly in crystalline form and are composed mainly by anglesite (lead sulphate), being the dominant element in them the Pb although present also relatively high levels of sulphates of, Ba, Ti and Fe. To note that changes in the composition of the raw material, does not influence the

mineralogical composition of the scales and therefore, the formation process of them is independent of the raw material used, only ilmenite or ilmenite and slag.

These scales are enriched in Ra isotopes with activity concentrations that can reach 2000 Bq/g of ^{228}Ra and 500 Bq/g of ^{226}Ra. If the radiometric determinations are performed sometime after collection, important corrections should be applied to fix the levels of the different radionuclides at zero time.

Although external gamma dose rates up to 12 μSv/h have been measured in the crystallizers where the scales are formed and accumulated, the very low occupancy factor of the area implies occupational and public doses lower than 1 mSv/y.

In addition, and due the high radon concentrations measured in crystallizers with their open doors (about 1000 Bq/m^3), a forced ventilation during the maintenance operations is needed to reduce the radon concentration up to 200 Bq/m^3, lower than reference value given by the European Union regulation (600 Bq/m^3) for working places.

In relation to the inhalation radiological doses, the most restrictive particulate matter concentrations (Cr) to be inhaled were 0.16 and 0.28 mg/m^3 for CS2 and CS3 samples, which guarantees that the annual committed dose for workers due to the inhalation of particular matter is lower than 1 mSv/y.

But scales samples also show a high concentration of stable Pb around 40%, that limits during the maintenance operations the air particulate matter concentrations of around 0.030 mg/m^3 for the samples with the higher concentration of Pb. These values are one order of magnitude lower than the corresponding ones for radiological risks (Cr), indicating that by inhalation, the Pb is the limiting element to take into account in the maintenance operations.

Acknowledgements: This research was partially supported by the Spanish Government Department of Science and Technology (MINECO) through the project "Fluxes of Radionuclides Emitted by the Phosphogypsum Piles Located at Huelva; Assessment of the Dispersion, Radiological Risks and Remediation Proposals" (Ref. CTM 2015-68628-R),), and the project of the Regional Government of Andalusia called “Basic processes regulating the fractionations and enrichments of natural radionuclides under acid mine drainage conditions” (Ref.: UHU-1255876) and the project of the University of Cadiz called "New methodogy of radioisotope isolation with environmental interest for its measurement by alpha spectrometry" (Ref: PR2019-024). The authors acknowledges to the staff of CITIUS at the University of Seville their help in the application of the X-ray techniques.

6. References

ATSDR.2007. Agency for Toxic Substances and Disease Registry. Toxicological profile for Barium. Atlanta, GA: U.S. Department of Health and Human Services, Public Health Service.

Beddow H., Black S., Read D. 2006. Naturally occurring radioactive material (NORM) from a former phosphoric acid processing plant. J Environ Radioact 86 (3), 289-312. https://doi.org/10.1016/j.jenvrad.2005.09.006

Bolívar J.P., Martín J.E., García-Tenorio R., Perez-Moreno J.P., Mas J.L. 2009. Behaviour and fluxes of natural radionuclides in the production process of a phosphoric acid plant. Appl Radiat Isotopes 67, 345–356. https://doi.org/10.1016/j.apradiso.2008.10.012

Chernet T. 1999. Applied mineralogical studies on Australian sand ilmenite concentrate with special reference to its behavior in the sulphate process. Miner Eng 12 (5), 485–495. https://doi.org/10.1016/S0892-6875(99)00035-7

Contreras, M, Martín, M. I., Gázquez, M. J., Romero, M., & Bolívar, J. P. 2014. Valorisation of ilmenite mud waste in the manufacture of commercial ceramic. Constr Build Mater, *72*, 31–40. https://doi.org/10.1016/j.conbuildmat.2014.08.091.

Directive 2003/88/EC of the European Parliament and of the Council of 4 November 2003 concerning certain aspects of the organisation of working time.

García-Tenorio R., Bolivar J.P., Gazquez M.J. and Mantero J. 205. Management of by-products generated by NORM industries: towards their valorization and minimization of their environmental radiological impact. Journal of Radioanalytical and Nuclear Chemistry 306, 641-648.

Gázquez M.J., Bolívar J.P., García-Tenorio R., Vaca F. 2009. Physicochemical characterization of raw materials and co-products from the titanium dioxide industry. J Hazard Mater 166:1429–1440. DOI: 10.1016/j.jhazmat.2008.12.067

Gázquez M.J., Bolívar J.P., Vaca F., García-Tenorio R., Caparros A. 2013. Evaluation of the use of TiO2 industry red gypsum waste in cement production. Cem Concr Compos. 37, 76-81. https://doi.org/10.1016/j.cemconcomp.2012.12.003

Gázquez M.J., Mantero J., BolívarJ.P., García-Tenorio R., Vaca F., Lozano R.L. 2011. Physico-chemical and radioactive characterization of TiO2 undissolved mud forits valorization. J Hazard Mater. 191, 269–276. https://doi.org/10.1016/j.jhazmat.2011.04.075

Genie 2000 3.0 Operations Manual (2004). Canberra Industries.

Godoy J. M. and Petinatti da Cruz R. 2003. Ra-226 and Ra-228 in scale and sludge samples and their correlation with the chemical composition. J Environ Radioact 70 (3), 199-206. DOI: 10.1016/S0265-931X(03)00104-8

Guerrero J.L., Pérez-Moreno S.M., Mosqueda F., Gázquez M.J., Bolívar J.P.2020. Radiological and physico-chemical characterization of materials from phosphoric acid production plant to assess the worker's radiological risks. Chemosphere, 253, 126682.https://doi.org/10.1016/j.chemosphere.2020.126682.

Hallstadius L.1984. A method for Electrodeposition of actinides. Nucl Instrum Meth 223, 226. https://doi.org/10.1016/0167-5087(84)90659-8

Harvey M. P., Hipkin J., Simmonds J. R., Mayall A., Cabianca T., Fayers C., Haslam I. 1994. Radiological Consequences of Waste Arising with Enhanced Natural Radioactivity Content from Special Metal and Ceramic Processes, Rep. EUR 15613, Office for Official Publications of the European Communities, Luxembourg.

Hartwell J.K., ARH-SA-215. Atlantic Richfield Handford Company. Richland. Washington, June 1975.Huijbregts, W.M.M., De Jong, M.P. Timmermans, C.W.M. 2000. Hazardous accumulation of radioactive lead on the water wall tubes of coal-fired boilers. Anti-corrosion Methods Mater. 7 5, 274–279. https://doi.org/10.1108/00035590010352368

IAEA 1999, International Atomic Energy Agency, International Labour Office. Assessment of Occupational Exposure Due to Intakes of Radionuclides, Safety Guide, SAFETY STANDARDS SERIES No. RS-G-1.2, Vienna (1999).

IAEA 2004, International Atomic Energy Agency. Methods for Assessing Occupational Radiation Doses Due to Intakes of Radionuclides, Safety Reports Series, 37, Vienna.

IAEA 2006. Assessing the Need for Radiation Protection Measures in Work Involving Minerals and Raw Materials. Safety Reports Series No 49

IAEA 2014 Radiation Protection and Safety of Radiation Sources: International Basic Safety Standards, General Safety Requirements, Safety Standards Series No. GSR Part 3. European commission, food and agriculture organization of the united nations, international atomic energy agency, international labour organization, OECD nuclear energy agency, pan American health organization, united nations environment programme, world health organization http://www-pub.iaea.org/MTCD/publications/PDF/Pub1578_web-57265295.pdf

IAEA. 2012. Safety Reports Series No.76. Radiation Protection and NORM Residue Management in the Titanium Dioxide and Related Industries. *IAEA Safety Standards and Related Publications*, 1–100.

ICRP, 1994. International Commission On Radiological Protection, Human Respiratory Tract Model for Radiological Protection ICRP Publication 66, Ann. ICRP 24 (1-3), 1994

Klepka M., Lawniczak-Jablonska K., Jablonski M., Wolska A., Minikayev R., Paszkowicz W., Przepiera A., Spolnik Z., Van Grieken R. 2005. Combined XRD, EPMAand X-ray absorption study of mineral ilmenite used in pigments production. J Alloy Compd. 401. 281–288. DOI: 10.1016/j.jallcom.2005.02.047

Landa Edward R. (2007). Naturally occurring radionuclides from industrial sources: characteristics and fate in the environment. Radioact Environ. 10. DOI: 10.1016/S1569-4860(06)10010-8

Lehritani M., Mantero J., Casacuberta N., Masqué P., García-Tenorio R.2012. Comparison of two sequential separation methods for U and Th determination in

environmental samples by alpha-particle spectrometry. 100 (7), 431-438. DOI: 10.1524/ract.2012.1933

Mantero J., Gazquez M.J., Bolivar J.P., Garcia-Tenorio R., Vaca F. 2013. Radioactive characterization of the main materials involved in the titanium dioxide production process and their environmental radiological impact. J Environ Radioact. 120, 26-32. DOI: https://doi.org/10.1016/j.jenvrad.2013.01.002

Mantero J., Gázquez M.J., Hurtado S., Bolívar J.P., García-Tenorio R. 2015. Application of gamma-ray spectrometry in a NORM industry for its radiometrical characterization. Radiat Phys Chem. 116, 78-81.

Mantero J., Thomas R., Isaksson M., Forssell-Aronsson, E., Holm E., García-Tenorio R. 2019. Quality Assurance via internal tests in a newly setup laboratory for environmental radioactivity. Journal of Radioanalytical and Nuclear Chemistry 322,891-900

Penfold, J.S.S., Mobbs, S.F., Degrange, J.-P., Schneider, T., Establishment of Reference Levels for Regulatory Control of Workplaces where Materials are Processed which contain Enhanced Levels of Naturally-Occurring Radionuclides, Radiation Protection 107, Office for Official Publications of the European Communities, Luxembourg (1999).

Pistorius P.C. and Coetzee C. 2003. Physicochemical aspects of titanium slag production and solidification. Metall Mater Trans B. 34B, 581–588. https://doi.org/10.1007/s11663-003-0027-8

Pownceby I.M., Sparrow J.G., Fisher-White J.M. 2008. Mineralogical characterisationof eucla basin ilmenite concentrates—first results from a new global resource. Miner Eng. 21, 587–597. https://doi.org/10.1016/j.mineng.2007.11.011

Technical Instruction (2011) of Nuclear Safety Council. (IS-33), on 21 December 2011 Radiological criteria for protection against exposure to natural radiation.

UNSCEAR 2008. United Nations Scientific Committee On The Effects Of Atomic Radiation. Report of the United Nations Scientific Committee on the Effects of Atomic Radiation, United Nations, New York.

WHO (World Health Organization) air quality guidelines for Europe, 2nd edition, 2000 273 pages ISBN 92 890 1358 3

Supplementary Materials

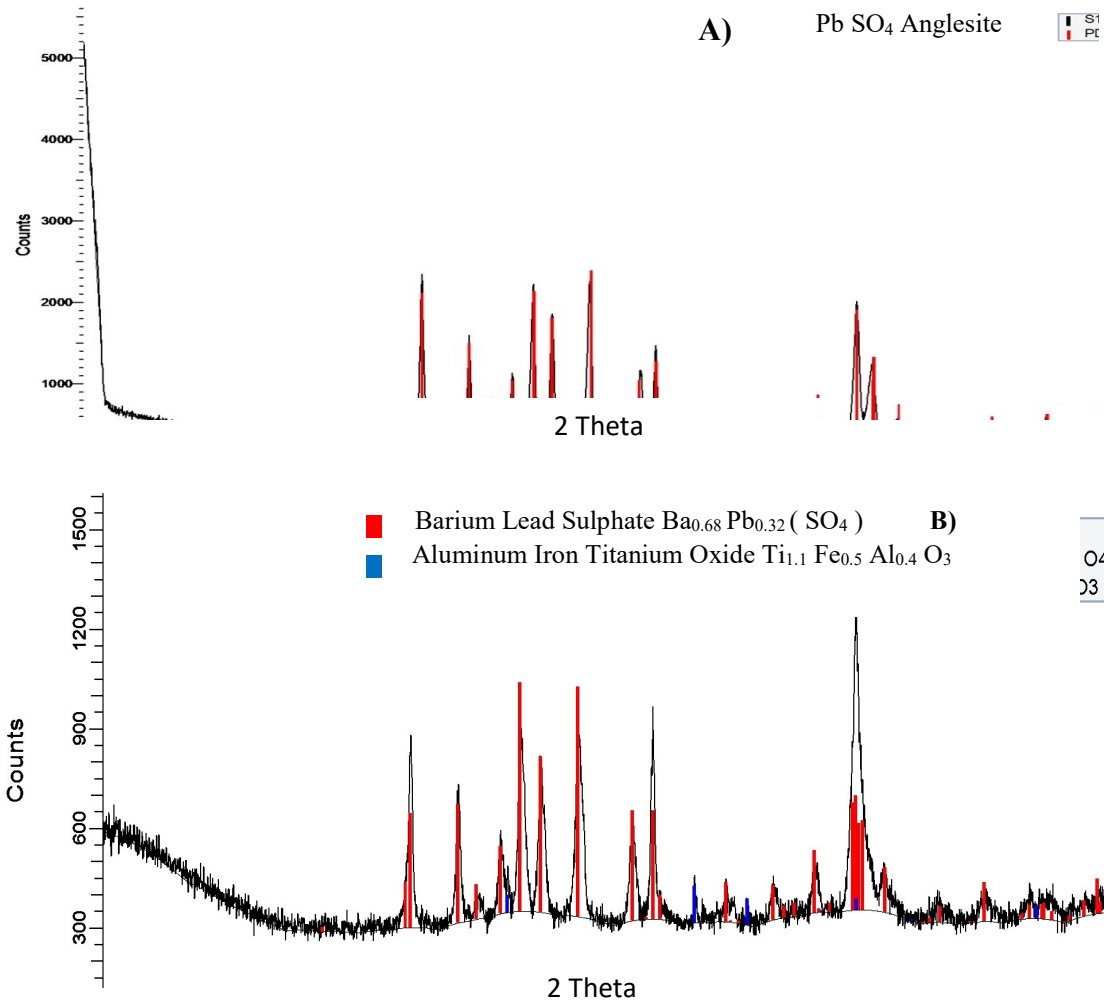

Figure S1. XRDs spectra corresponding to CS1 sample A) and IS B).

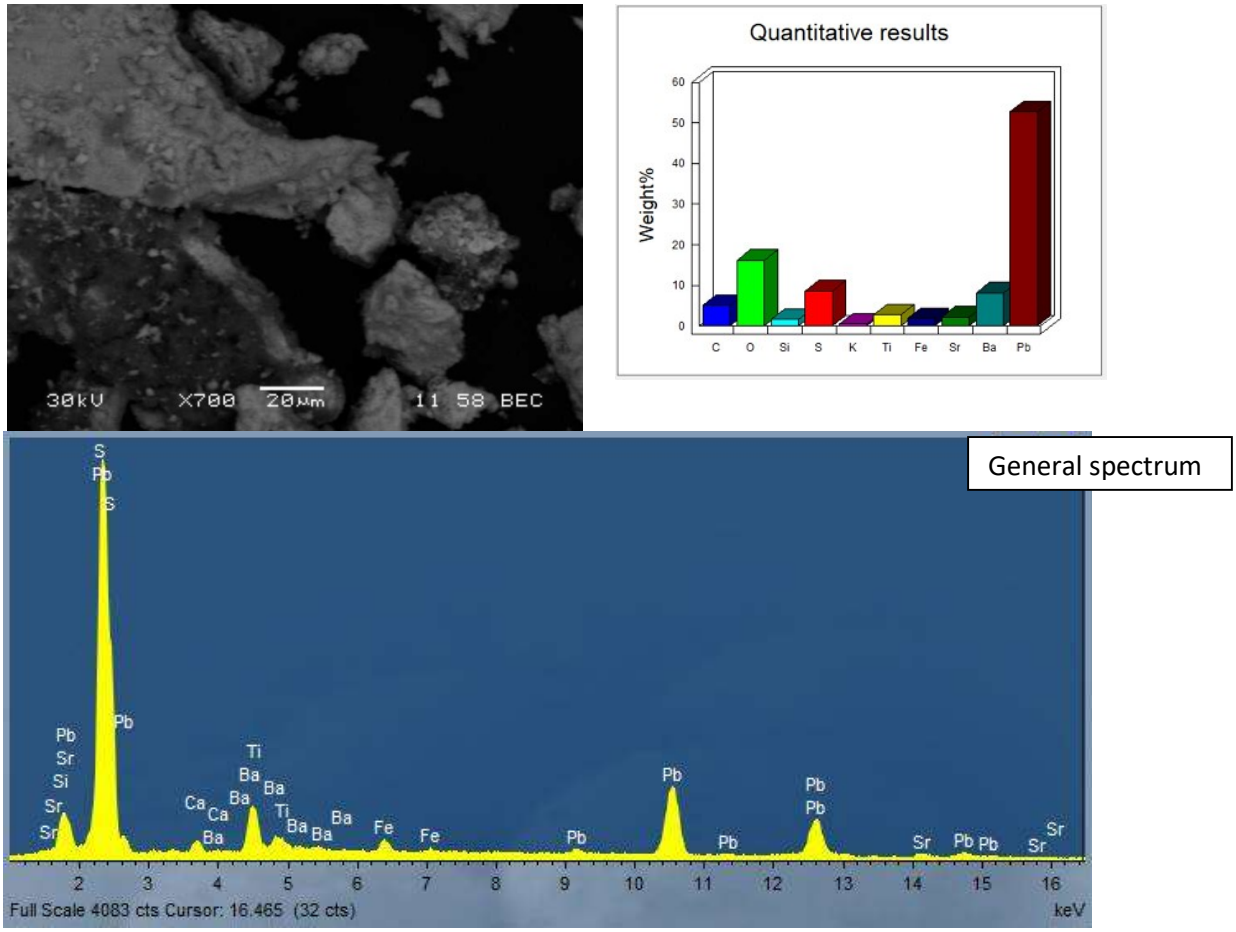

Figure S2. Representative SEM for CS samples, quantitative results and EDX spectrum.

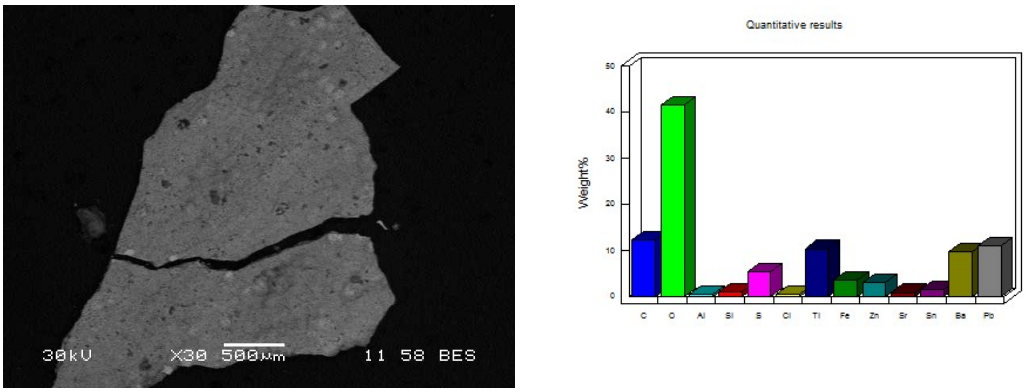

Figure S3. Representative SEM image of IS sample and the quantitative results.

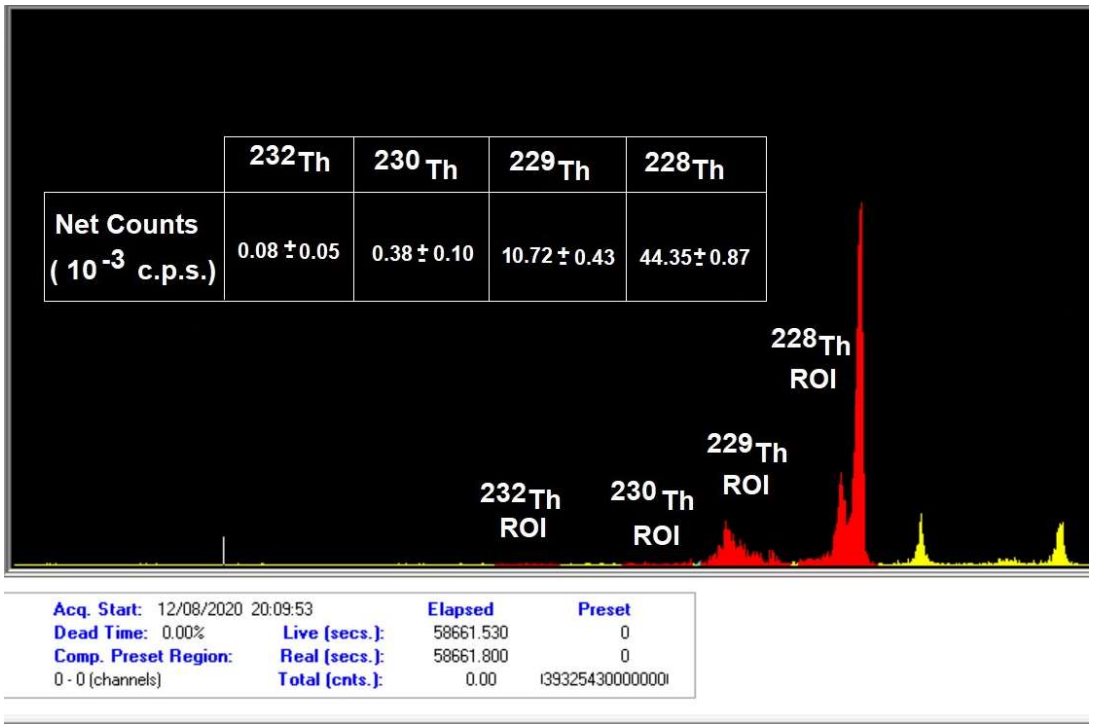

Figure S.4 Screenshot of a Th spectrum (belonging to one of the three replicates of sample CS3). Marked In red, the Region Of Interest (ROI) for the different Th radionuclides where the net counts (in millicounts per second) after background subtraction are calculated.

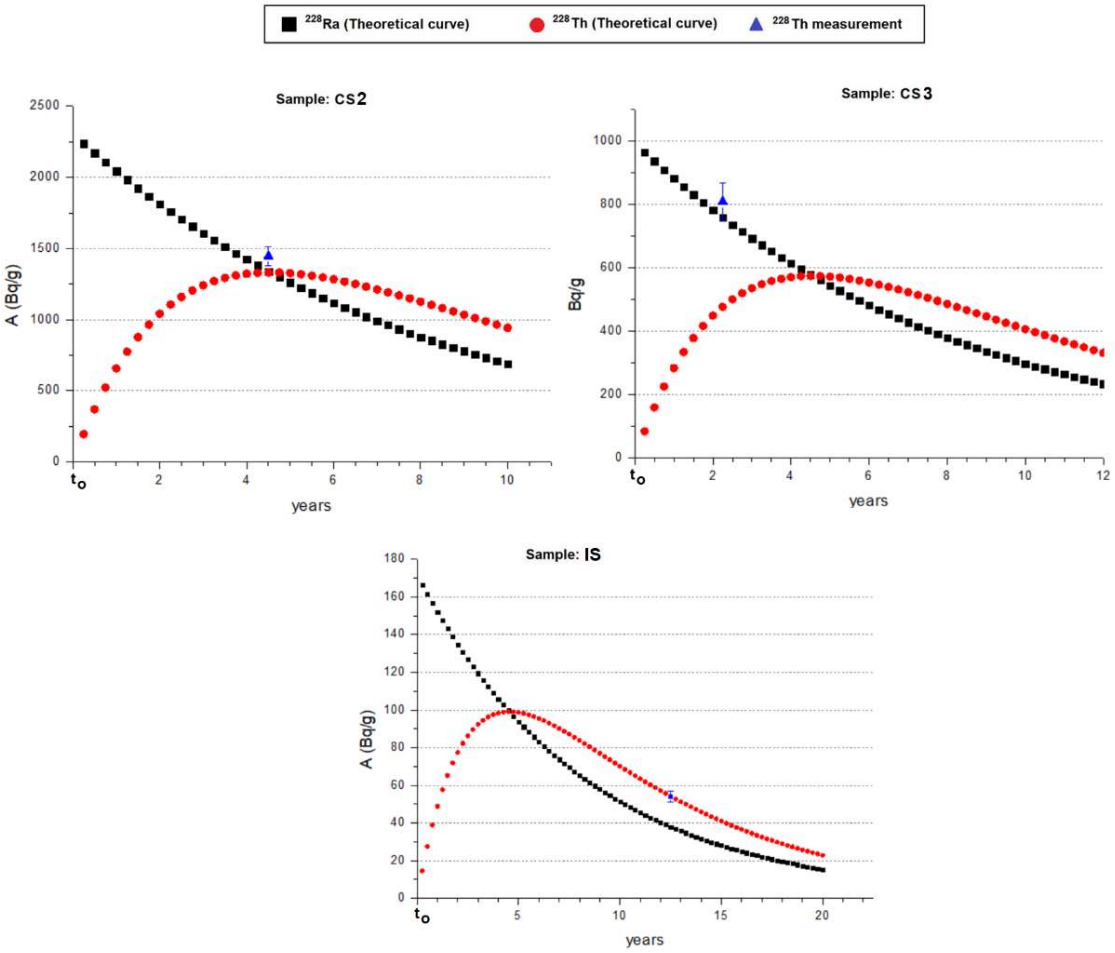

Figure S5.- Estimated temporal evolution of the activity concentrations of ^{228}Ra and ^{228}Th of three of the samples analyzed, together with the values obtained for ^{228}Th in the experimental measurements by gamma-ray. Note that sample CS3 is the only sample that does not fulfill all hypothesis in the assessments of these curves and, as a consequence, theoretical and experimental values do not match.

Table S1. Natural decay series, radionuclides, gamma energies and gamma spectrometry MDA for the XtRa system (after 200000 s measurements).

Natural Series	Radionuclide	Energy (keV)	MDA (Bq)
^{238}U	^{234}Th	63.3	0.60
	^{234m}Pa	1001	12.1
	^{214}Pb	295.2 and 351.9	0.38
	^{214}Bi	609.3, 1120.3 and 1764.5	0.30
	^{210}Pb	46.5	0.55
^{232}Th	^{228}Ac	338.3, 911.2 and 969	0.66
	^{224}Ra	241	1.30
	^{212}Pb	238.6	0.40
	^{212}Bi	727.3	2.81
	^{208}Tl	583.2 and 2614.5	0.24

Table S2. Thorium series: Activity concentrations of ^{228}Ra and ^{228}Th determined by gamma-ray spectrometry and of ^{228}Th determined by alpha-particle spectrometry, in each case at the time of their measurement.

Sample	Collection date (t_0)	Gamma spectrometry (Bq/g)			Alpha spectrometry (Bq/g)	
		Measurement date (t_m)	^{228}Ra (t_m)	^{228}Th (t_m)	Measurement date (t_m)	^{228}Th(t_m)
CS1	DEC-2006	SEP-2019	40 ± 6	63 ± 8	AUG-2020	63 ± 5
CS2	MAY-2016	SEP-2018	1662 ± 50	1420 ± 80	AUG-2020	1446 ± 64
CS3	*MAY- 2016*	*0CT-2018*	725 ± 25	810 ± 56	*AUG-2020*	400± 10
MF	DEC-2006	JUN-2013	29.3 ± 3.5	38.2 ± 2.1	AUG-2020	15 ± 2
IS	DEC-2006	APR-2014	70 ± 3	96 ± 8	AUG-2020	17.5 ± 1.2

Table S3. Uranium series: Activity concentrations of ^{226}Ra and ^{210}Pb determined by gamma-ray spectrometry (Bq/g) and of ^{238}U and ^{234}U determined by alpha-particle spectrometry (Bq/kg), in each case at the time of their measurement (t_m). Measurement dates for U-isotopes are not relevant due to their huge half-lifes.

Sample	Collection date (t_0)	Gamma spectrometry (Bq/g)			Alpha spectrometry (Bq/kg)	
		Measurement date (t_m)	^{226}Ra	^{210}Pb	^{238}U	^{234}U
CS1	DEC-2006	SEP-2019	121 ± 6	108 ± 9	52 ± 7	87 ± 6
CS2	MAY-2016	SEP-2018	448 ± 24	326 ± 21	41 ± 5	98 ± 7
CS3	MAY- 2016	0CT-2018	190 ± 8	251 ± 20	150 ± 18	172 ± 20
MF	DEC-2006	JUN-2013	14.4 ± 0.6	5.5 ± 0.9	< 5.0	<5.8
IS	DEC-2006	APR-2014	1281 ± 40	1480 ± 80	44 ± 4	51 ± 4

Table S4. Radiological (Cr) and chemical (Cc) particulate matter concentration values (mg/m^3). Maximum quantity (mg) for which the radiological (Pr) and chemical (Pc) limits, are not exceeded

	CS1	CS2	CS3	IS	MF
Pr (mg)	317	19	34	72	714
Cr (mg/m^3)	2.64	0.16	0.28	0.60	5.95
Pc (mg)	3.3	4.3	3.9	8.3	125
Cc (mg/m^3)	0.027	0.036	0.033	0.069	1042